Application of a coil-type TDR probe for measuring the volumetric water content in weathered granitic bedrock

Shin'ya Katsura, Ken'ichirou Kosugi, and Takahisa Mizuyama

Department of Forest Science, Graduate School of Agriculture, Kyoto University, Kyoto, Japan

Corresponding author

Shin'ya Katsura

Laboratory of Erosion Control, Department of Forest Science

Graduate School of Agriculture, Kyoto University,

Kitashirakawa Oiwakecho, Kyoto 606-8502, Japan

Tel: +81-75-753-6090

Fax: +81-75-753-6088

E-mail: katsura3@kais.kyoto-u.ac.jp

Abstract

As a first step toward describing water flow processes in bedrock, we prepared a coil-type TDR probe capable of measuring volumetric water content, θ, in weathered bedrock at three depths. Because the coil-type TDR probe is large in diameter (19 mm), it can be installed even in highly weathered bedrock more easily and appropriately than conventional TDR probes that consists of two or three rods of small diameter (5-8 mm). The probe calibrations suggest that the values measured by the probe are very sensitive to changes in θ. Using the calibrated probe together with commercially available profile soil moisture sensors, we monitored the θ profile for 1 year. Even rainfall events with relatively small cumulative rainfall of 15 mm increased the bedrock θ, and the increments were comparable to those in the soil. After the end of the rainfall events, the bedrock θ displayed a more rapid drop than the soil, and varied little during the period of no rainfall. The water storage showed similar tendencies. These observations suggest that the bedrock θ is controlled by clearly distinguishable macropores and micropores within the bedrock. We conclude that the coil-type TDR probe is very effective in determining θ in weathered bedrock, and that bedrock, conventionally defined by conducting cone penetration tests and treated as impermeable, does conduct and hold

substantial amounts of water, and therefore contribute greatly to hydrological processes in headwater catchments.

Keywords

Volumetric water content

TDR technique

Coil-type

Bedrock

Weathered granite

1. Introduction

Recent studies in hillslope hydrology indicate that rainwater can infiltrate into bedrock, which had been conventionally treated as an impermeable layer (e.g., Okimura *et al*., 1985; Hiramatsu *et al*., 1990), and that bedrock groundwater can influence both the water budget and material balance in headwater catchments. Terajima *et al*. (1993) examined the water balance in two small catchments in granitic mountainous areas, and demonstrated that at least 18% of the annual precipitation percolated into bedrock. Groundwater that had infiltrated into bedrock then discharged very slowly, sustaining base flow and determining its chemistry (e.g., Inokura and Yoshimura, 1992; Mulholland, 1993; Komatsu and Onda, 1996; Burns *et al*., 1998). More recently, sprinkling experiments performed at the CB1 catchment in Oregon (Anderson *et al*., 1997a, 1997b; Montgomery *et al*., 1997, 2002) have shown that bedrock groundwater can also contribute to storm runoff generation and its chemistry. Many studies have also noted that bedrock groundwater flow plays significant role in the occurrence of landslides (e.g., Onda *et al*., 1999; Kato *et al*., 2000; Montgomery *et al*., 2002).

Previous studies on bedrock groundwater (e.g., Asano *et al*., 2003; Miyata *et al*., 2003; Uchida *et al*., 2003a, 2003b), including those cited above, have typically involved detailed hydrological,

hydrochemical, and thermal measurements of water already discharged from bedrock; few have examined water flow processes within bedrock because it is very difficult to access bedrock, which is often overlain by thick soil layers. Indeed, while previous studies have successfully emphasized the importance of bedrock groundwater in headwater catchments, physical descriptions of water movement processes within bedrock are needed to evaluate the effects of bedrock groundwater on runoff generation and water chemistry, and to predict timing and locations of landslide occurrences.

A few studies directly demonstrating processes of bedrock groundwater flow have been conducted by installing tensiometers and piezometers into bedrock (Wilson and Dietrich, 1987; Terajima and Moroto, 1990; Onodera, 1991; Montgomery *et al*., 1997; Kosugi *et al*, 2006). While these observations could address pressure head distribution within bedrock and thereby describe bedrock groundwater flow vectors during and after rainfall events, they could not provide absolute values and variation of water content within bedrock, which are required for evaluating the effects of bedrock on hydrological phenomena such as rainwater infiltration and storage. For a better understanding of hydrological processes in headwater catchments, including bedrock, it is important for water content within bedrock to be easily measured.

Time domain reflectometry (TDR) is a well established and widely used technique for determining water content in soils. Recently, some studies have attempted to apply this technique to measuring the water content in rock (Hokett *et al*., 1992; Schneebeli *et al*., 1995; Gimmi *et al*., 1997). They used conventional TDR probes with two or three parallel rods and installed them into fresh rocks by drilling guide holes to fit the rods. Whereas conventional probes are readily applicable to tight rocks with very low porosity (typically <<10%), application to highly weathered bedrock, located just below the soil layer and contributing largely to hydrological processes in headwater catchments, is somewhat uncertain because weathering has made the rock fabric and structure weak and fragile and therefore suitable accurately spaced guide holes are difficult to drill. Sasaki *et al*. (1998) applied conventional TDR probes to a variety of rocks with relatively large effective porosity (>20%), demonstrating that a slight gap between the probe and rock can cause inaccurate measurements, especially for saturated or nearly saturated rock specimens. Therefore, in this study we instead used a coil-type TDR probe, newly developed by Nissen *et al*. (1998) and practically used to measure the water contents in soils (Vaz and Hopmans, 2001; Tsutsumi, 2003; Kosugi *et al*., 2004), as a potentially more effective tool. Because a coil-type TDR probe is larger in diameter than

conventional TDR rods, it can be installed and measure the water content more easily and appropriately even in highly weathered bedrock.

The objectives of this study were to verify that a coil-type TDR probe can provide an effective technique to measure water content in weathered bedrock, determine bedrock water content in the field using this technique, and elucidate water movement processes in weathered bedrock at the study site.

2. Materials and methods

2.1 Details of a coil-type TDR probe

The TDR technique is based on the dependency of an electromagnetic wave velocity on the dielectric constant of the medium propagating the wave. A waveguide is inserted into the medium, and an electromagnetic wave generated by a time domain reflectometer travels along the waveguide. The wave is reflected at the beginning and end of the waveguide, and the wave velocity v can be

1 determined by measuring the time required for the wave to travel between the beginning and end of
2 a waveguide of known length. When the waveguide is inserted into the medium with the relative
3 dielectric constant of κ, the relationship between v and κ can be expressed as

4 $$\kappa^{1/2} = c / v \equiv \alpha \qquad [1]$$

5 where c is the velocity of an electromagnetic wave in free space (3×10^8 m s^{-1}) (Robinson *et al.*,
6 2003). Hereafter, we define the value $\kappa^{1/2}$ as α.

7 In this study the medium corresponds to bedrock, which consists of solid materials, air, and
8 water. Each of these three components contributes to the relative dielectric constant of the whole
9 bedrock $\kappa_{Bedrock}$ according to its volume fraction. This relationship can be described
10 semi-theoretically by the three-phase mixing model (Nissen *et al.*, 1998; Vaz and Hopmans, 2001):

11 $$\kappa_{Bedrock} = \left[\theta\kappa_w^n + (\phi - \theta)\kappa_a^n + (1-\phi)\kappa_s^n\right]^{\frac{1}{n}} \qquad [2]$$

12 where θ and ϕ are the volumetric water content and the porosity of bedrock, respectively; κ_w, κ_a, and
13 κ_s are the relative dielectric constants of water, air, and solid materials, respectively; and n is the
14 parameter that summarizes the geometry of the medium (i.e., bedrock) with relation to the applied
15 electric field and varies from –1 in the case where the electric field is perpendicular to 1 in the case

where the electric field is parallel to layers of dielectrics (Roth *et al*., 1990). Since κ_w (80.16 at 20°C) is much larger than both κ_s (range, 3-7) and κ_a (1) (Handbook of Chemistry, 2004), $\kappa_{Bedrock}$ strongly depends on the bedrock volumetric water content θ. Hence the bedrock volumetric water content θ can be determined by measuring α in Eq. [1], which reflects $\kappa_{Bedrock}$ expressed in Eq. [2].

We made a coil-type TDR probe capable of measuring water content at three depths; the detailed diagram is shown in Fig. 1. Three coaxial cables, the ends of which were individually connected with two stainless wires (0.3 mm in diameter), were inserted inside a 149-mm-long PVC column (19 mm in external diameter and 13 mm in internal diameter). These coaxial cables were individually connected to a time domain reflectometer (TDR100; Campbell Scientific, Logan, UT, USA) that generates an electromagnetic wave with a short rise time and analyzes a reflected electromagnetic waveform. The wires connected to the cables were taken from the PVC column via small holes drilled into the PVC column, and individually coiled 40 mm apart around the surface of the PVC column. Note that no stainless wire ever crosses the others. These coiled wires act as waveguides and sensors detecting the water content. They guide an electromagnetic wave generated by the time domain reflectometer and the wave is reflected at the beginning and end of the wires, and the

1 waveform is sampled and analyzed by the reflectometer. The top and bottom of the PVC column
2 were closed completely with silicone sealant (Cemedine 8060; Cemedine, Tokyo, Japan) to prevent
3 water from leaking into the PVC column. Finally the probe was entirely coated by a thick PVC sheet
4 to protect the wires.

5 Compared to conventional TDR probes, a coil-type TDR probe has two major advantages
6 derived from the coiled waveguides, which are markedly longer than the probe itself; i.e., they
7 provide high resolution and small volume of influence (Nissen *et al*., 1998). In this study, the larger
8 diameter of the coil-type probe (19 mm) than that of conventional probe rods (5-8 mm) had another
9 advantage; it is far easier to drill one guide hole of a large diameter to fit the coil-type probe than to
10 drill two or three smaller, accurately spaced guide holes to fit conventional probe rods into highly
11 weathered bedrock.

12

13 **2.2 Calibration of the coil-type TDR probe**

14

15 In the case of conventional TDR probes, the measured value α is directly related to κ by Eq. [1],

and therefore the well-known calibration equation developed by Topp *et al*. (1980) can be applied. The value of α measured by the coil-type probe, however, includes the effects not only of the medium into which the probe is inserted (i.e., weathered bedrock) but also of the probe materials; i.e., the dielectric constant of both bedrock and the probe materials influence the value α. This in turn demonstrates the need for a calibration of each sensor individually.

We performed the following calibration procedures. Because we had confirmed that the medium located within a radius of 25 mm from the center of each sensor affects the measured value α, we prepared a PVC cylinder 145 mm in length and 58 mm in diameter; this cylinder had been previously cut into three segments: 50, 40, and 55 mm long from the top to the bottom. The coil-type TDR probe was inserted into the center of the reassembled cylinder so that the center of one sensor was situated at the center of each segment, and the air-dried bedrock materials sampled and crushed at the study site filled the space between the probe and the cylinder wall. Five measurements were taken for each sensor, from which the maximum and minimum values were excluded, and the value of α was calculated by taking the average of the remaining three values. After the measurements, the cylinder was carefully separated into three segments, and the weight of the bedrock materials within

each segment was measured individually. Then the materials were oven-dried over 24 h, and the weight was again measured to calculate the volumetric water content θ in each segment. These procedures were repeated with several increments of increasing water content in the bedrock materials. Finally a third-order polynomial equation was fitted to the observed relationship between α and θ for each sensor, used as a calibration equation to compute θ from α.

2.3 Study site and field observations

Field measurements of the water contents were performed in the Kiryu experimental basin (5.99 ha) in Shiga Prefecture, central Japan (Fig. 2). The mean annual air temperature was 13.6°C (1997-2004), with the highest average monthly temperature (24.9°C) in August and the lowest (2.9°C) in January. The mean annual precipitation was 1645.4 mm (1972-2004), most of which fell as rain. Annual evapotranspiration in the Kiryu experimental basin ranged from 609.4 to 944.0 mm, the equivalent of 35.4 to 65.6% of the annual precipitation (1972-2003).

The Akakabe catchment, located in the southeastern part of the Kiryu experimental basin, was

chosen for this study (Fig. 2). This catchment has an area of 0.086 ha and a mean gradient of 22.0°; it is predominantly covered with Japanese cypress (*Chamaecyparis obtusa*) planted in 1959. The catchment is underlain by granitic bedrock; this granite is called Tanakami Granite (Collaborative Research Group for the Granites around Lake Biwa, 2000), and has a primary mineral composition consisting mainly of quartz, alkali feldspars, plagioclase feldspars, and biotite (Torii, 1996).

We installed the calibrated coil-type TDR probe at the point indicated by a solid circle in Fig. 2. The soil depth to bedrock at this point was determined using a cone-penetrometer with a cone diameter of 30 mm, a weight of 5 kg, and a fall distance of 50 cm. The result of the cone penetration test at this point is shown in Fig. 3. The N_c value in Fig. 3 denotes the number of blows required for a 10-cm penetration. Many previous studies have suggested that bedrock be defined as the layer with the N_c value exceeding 50 for granitic regions (Okunishi and Iida, 1978; Okimura and Tanaka, 1980; Mochiduki and Matsumoto, 1986); we also adopted this definition. The N_c value at this point sharply increased to more than 50 at a depth of approximately 50 cm (Fig. 3), indicating that the soil depth at this point was 50 cm.

Figure 4 shows a photograph of the soil-bedrock interface observed at a pit dug for the coil-type

TDR probe installation. The depth of 50 cm at the installation point corresponded to the soil-bedrock interface that could be recognized relatively clearly by visual examination. The surface of the bedrock was not sufficiently weathered to be considered saprolite, and it could be crushed into small fragments with bare hands while retaining rock fabric and structure.

Previous studies conducted in the Akakabe catchment indicate that bedrock infiltration is a very important hydrological process in this catchment. For example, Kosugi *et al*. (2006) examined the water balance for an unchanneled 0.024-ha catchment in the Akakabe catchment (indicated by the shaded area in Fig. 2), and demonstrated that about 35% to 55% of annual precipitation infiltrates into the bedrock. They also measured pressure head distribution in the unchanneled catchment using 22 soil (10 to 94 cm deep from the ground surface) and 10 bedrock tensiometers (9 to 78 cm deep from the soil-bedrock interface), suggesting that all the rainwater infiltrate into the bedrock in the middle slope and upslope regions in the catchment. Katsuyama *et al*. (2004) conducted detailed hydrological and hydrochemical observations in the same unchanneled catchment and suggested that the groundwater flow passing through the bedrock keeps the NO_3^- concentrations of the baseflow from the Akakabe catchment very low. Katsura *et al*. (2006) determined the saturated hydraulic

conductivity of the shallow bedrock layer, located within 17 cm from the bedrock surface at a point indicated by a grey circle in Fig. 2, as 1.0×10^{-4} cm s^{-1}, which corresponds to the rainfall intensity of as high as 3.6 mm hr^{-1}. These previous findings obtained in the Akakabe catchment emphasize the importance of direct measurements of the bedrock water content to quantify rainwater infiltration processes into and water storage properties in the bedrock in this catchment.

After eliminating the soil layer at the point, we drilled a hole (approximately 150 mm in length and 20 mm in diameter) in the bedrock using an electric drill to achieve minimum disturbance, into which the calibrated coil-type TDR probe was inserted. The diameter of the probe was equivalent to that of the drill bit, ensuring good contact between the probe and the surrounding bedrock (Fig. 5). The top of the probe, situated at the depth corresponding to the soil-bedrock interface, was covered with epoxy resin to prevent water from flowing from the top and along the probe (see also Fig. 4). Using the installed probe, we monitored the bedrock water content at depths of 3, 7, and 11 cm from the bedrock surface (referred hereafter to as θ_{B3}, θ_{B7}, and θ_{B11}, respectively). Note that the coil-type probe measurement can be considered close to a point measurement (Nissen *et al*., 1998).

We also installed profile soil moisture sensors (EasyAG; Sentek Sensor Technologies, Adelaide,

SA, Australia) above the exact point of the coil-type probe installation according to the manufacturer's instructions. The EasyAG sensors can determine soil water content at 10-cm intervals. In this study, we monitored the soil moisture at depths of 10, 20, 30, and 40 cm from the ground surface (referred to hereafter as θ_{S10}, θ_{S20}, θ_{S30}, and θ_{S40}, respectively). We used the default nonlinear calibration equation, established for sands, loams, and clay loams by the sensor maker, to calculate the soil water content from the measured value.

The installation of the coil-type TDR probe into the bedrock inevitably disturbed the overlying soil layer considerably. Hence we used the data obtained from 1 June 2003 to 31 May 2004 for the following discussions and analyses although the probe was installed on 31 October 2001; it was expected that the influence of soil disturbance around the measurement point caused by the probe installation would dissipate during the period of 19 months (i.e., November 2001-May 2003).

3 Results

3.1 Calibrations of the coil-type TDR probe

Figure 6 shows the observed relationships between α and θ for the individual sensors. The measured value α rose as θ increased, and the fitted third-order polynomial equations adequately describe the tendencies of the observed relationship. The calibration equations to compute θ_{B3}, θ_{B7}, and θ_{B11} were determined as follows, respectively:

$$\theta_{B3} = 0.246\alpha^3 - 2.387\alpha^2 + 7.827\alpha - 8.448 \quad [3]$$

$$\theta_{B7} = 0.296\alpha^3 - 2.956\alpha^2 + 9.973\alpha - 11.103 \quad [4]$$

$$\theta_{B11} = 0.086\alpha^3 - 1.001\alpha^2 + 4.012\alpha - 5.016 \quad [5]$$

These equations yield negative values of θ in the range of α less than approximately 2.4, but we confirmed that the values of α measured in the field never fell into this range.

Water content values calculated using Eqs. [3]-[5] involved a relatively large range of variation (approximately ±0.02) even in the period when no rain was observed and rapid change in water content would not be expected. Therefore we took the 30-min moving averages of the water contents measured at a 5-minute interval at each depth (Fig.7) and used them as θ in the following figures and discussions.

1

2 **3.2 Annual variations in the soil and bedrock water contents**

3

4 Figure 8 shows the variations in the soil and bedrock water content throughout the observation

5 period (1 June 2003-31 May 2004). The bedrock water content ($\theta_{Bedrock}$), as well as the soil water

6 content (θ_{Soil}), rose substantially in response to rainfall, but $\theta_{Bedrock}$ displayed little response to

7 rainfall from December 2003 through mid-February 2004. After the end of each individual rainfall

8 event that produced a rise in $\theta_{Bedrock}$, $\theta_{Bedrock}$ sharply dropped and soon exhibited relatively constant

9 values, whereas θ_{Soil} declined gradually.

10 Figure 9 summarizes the annual variation in both the soil and bedrock water content. The

11 difference between the maximum and minimum values of the water content throughout the

12 observation period ranged from 0.159 (θ_{B11}) to 0.290 (θ_{B3}) for the bedrock (average, 0.232), and

13 from 0.175 (θ_{S10}) to 0.275 (θ_{S20}) for the soils (average, 0.243), suggesting that the range of the water

14 content variation in the bedrock was nearly as large as that in the soil. However, $\theta_{Bedrock}$ was

15 concentrated in a very narrow range compared to θ_{Soil}; i.e., the range between the 25th and 75th

1 percentiles was narrower for the bedrock than for the soil. This tendency is emphasized in Fig. 10 in
2 which the relative frequencies of $\theta_{Bedrock}$ show a larger kurtosis than those of θ_{Soil}.
3
4 **3.3 Temporal variations in the soil and bedrock water content during rainfall events**
5
6 Figures 11a-13a show the detailed variation in the water content profile observed during rainfall
7 events. Here we have defined separate individual rainfall events as delimited by a period of more
8 than 1 day without rainfall, and used the same definition in the following figures and discussions.
9 The contour lines of the increments in the water content compared with those at beginning of rainfall
10 are also shown in Figs. 11b-13b.
11 During a small rainfall event (total rainfall 19.7 mm; Fig. 11), θ_{Soil} increased from the
12 shallowest layer progressively with depth, but $\theta_{Bedrock}$ showed little response. After the end of the
13 event, θ_{Soil} fell very gradually. On the other hand, a medium-sized rainfall event (total rainfall 51.5
14 mm; Fig. 12) generated a significant rise in the water content in the soils through the bedrock. While
15 the water content in the shallower soil layer (θ_{S10} and θ_{S20}) changed in relatively clear response to

rainfall intensity, little correspondence between water content in deeper soil layers (θ_{S30} and θ_{S40}) and the rainfall intensity could be recognized. The $\theta_{Bedrock}$ suddenly rose at 18:30 h on 29 November and dropped more sharply than θ_{Soil}. Note that θ_{B11} continued to vary little from 18:30 h on 29 November through 08:00 h on 30 November.

During a large rainfall event (total rainfall 160.6 mm; Fig. 13), both θ_{Soil} and $\theta_{Bedrock}$ again rose dramatically. The θ changed more gradually as the depth increased in both the soil and bedrock layer. The $\theta_{Bedrock}$ again rose sharply, especially around 10:00 h on 16 May, followed by relatively constant values for approximately 14 h; it then dropped more steeply than θ_{Soil}.

4 Discussion

4.1 Usefulness of the coil-type TDR probe to measure water content in weathered bedrock

The calibration results (Fig. 6) indicate that the value of α measured by the coil-type TDR probe is strongly dependent on the water content θ in the surrounding medium and therefore can detect

1 even a very small change, e.g., 0.01, in θ. We installed the calibrated probe in the bedrock at the
2 study site. The larger diameter of the coil-type TDR probe contributed not only to easier installation
3 of the probe but also to good contact between the probe wall and the surrounding bedrock (Fig. 5).
4 Using the accurately calibrated and appropriately installed probe, we successfully measured the
5 water contents in the weathered bedrock at the study site (Figs. 8-13).

6 From the above discussions, together with the advantages of the coil-type TDR probe mentioned
7 in the previous section, it can be concluded that the use of coil-type TDR probe is an effective
8 technique for measuring the water content in highly weathered bedrock. It should be noted, however,
9 that we had to take 30-min moving averages of the water content calculated from the measured value
10 α to partially smooth out large variations that were found especially during the no-rainfall periods
11 (Fig. 7).

12

13 **4.2 Rainwater infiltration into the soil and bedrock**

14

15 The results shown in Figs. 11-13 suggest that rainwater generally infiltrates from the shallower

to deeper layers, and that increasing cumulative rainfall generates infiltration into the bedrock. Figure 14 directly exhibits the relationship between the total rainfall observed in individual events and the maximum depth at which water content showed response to the rainfall event. Here, we assumed that the water content responded to the event when its value increased more than 0.03 in comparison with a value just before the event. As shown in Fig. 14, larger cumulative rainfall induced infiltration into the deeper layer. The figure also shows that a relatively small cumulative rainfall, such as 15 mm, could produce bedrock infiltration. Moreover, for almost all of the events that caused bedrock infiltration, the infiltration front did not stop at the 3- or 7-cm depths from the soil-bedrock interface, but expanded to at least 11-cm depth, the maximum measurement depth in this study, indicating the high value of water diffusivity in the bedrock. Figure 14 also suggests that the tendencies mentioned above are influenced very little by antecedent moisture conditions in the surface soil layer (i.e., θ_{S10}).

Figure 15a-g shows the relationship between the maximum increment in water content ($\Delta\theta_{max}$) and the cumulative rainfall observed before the maximum water content was observed at each depth. As shown in Fig. 14, deeper layers generally required larger cumulative rainfall to attain substantial

$\Delta\theta_{max}$, such as 0.03, and cumulative rainfall of more than approximately 15 mm could produce bedrock infiltration. In addition, larger cumulative rainfall values increased the values of $\Delta\theta_{max}$ at each depth, but cumulative rainfall beyond 50 mm no longer increased $\Delta\theta_{max}$ at 7- and 11-cm depths from the soil-bedrock interface (Fig. 15f and g, respectively) probably because the bedrock at these depths reached full saturation. Again, the tendencies mentioned above were barely influenced by the antecedent moisture conditions at each depth.

For Fig. 15h, we have computed the maximum increments in the average water content weighted by the thickness, $\Delta\theta_{ave,\ max}$, for the whole soil layer (50 cm thick) and shallow bedrock layer (13 cm thick). Figure 15h suggests that the values of $\Delta\theta_{ave,\ max}$ for the soil layer increased as the cumulative rainfall increased. On the other hand, $\Delta\theta_{ave,\ max}$ for the bedrock layer was nearly zero in the smaller cumulative rainfall range, but sharply increased in the range where the cumulative rainfall was more than 15 mm and less than 45 mm, and no longer increased in the larger cumulative rainfall range. This resulted in the values of $\Delta\theta_{ave,\ max}$ for the bedrock layer as large as or even larger than those for the soil layer in the range where the cumulative rainfall was more than 15 mm.

The observation results that $\theta_{Bedrock}$ markedly rose in response to rainfall events (Figs. 8, 12-15)

clearly indicate that bedrock infiltration in the study site occurred under unsaturated conditions. This supports the results and discussions by Kosugi *et al*. (2006); unsaturated infiltration into the bedrock is the dominant water flow process in the middle-slope region, including the measurement point in this study (Fig. 2), in the Akakabe catchment, which is underlain by weathered granitic bedrock.

4.3 Water storage in the soil and bedrock

Here we discuss how the bedrock layer at the study site contributes to rainwater storage. To evaluate the effects of antecedent rainfall, which is highly relevant to water storage, we employ the antecedent precipitation index *API*. An *API* with the half-life of *M* hours at the time *t* ($API_M(t)$) is calculated as

$$API_M(t) = API_M(t-1)\exp(\ln 0.5/M) + R(t)\exp(\ln 0.5/2M) \quad [12]$$

where $R(t)$ is the 1-h rainfall at time *t* (Suzuki and Kobashi, 1981). The effects of employing an antecedent precipitation index with short and long half-life values, API_{12} and API_{120}, are shown in Fig. 16a. Figure 16b shows the annual variation in the water storage (i.e., the total water volume

held) in both the 50-cm-thick soil layer (S_{Soil}) and the 13-cm-thick bedrock layer ($S_{Bedrock}$). Figure 16c displays the average water content, θ_{ave}, calculated by dividing S_{Soil} and $S_{Bedrock}$ by the thickness, of the corresponding soil and bedrock layer.

Both S_{Soil} and $S_{Bedrock}$ rose during rainfall events, but after the events, the former decreased gently while the latter dropped rapidly (Fig. 16b). The θ_{ave} showed similar tendencies (Fig. 16c). In addition, Fig. 16c suggests that the bedrock layer held more water than the soil layer of the same thickness throughout the year, especially during no-rainfall periods. Furthermore, comparisons among Fig. 16a, b, and c demonstrate that S_{Soil} and θ_{ave} in the soil layer have a good correspondence with a long half-life *API*, such as API_{120}, whereas $S_{Bedrock}$ and θ_{ave} in the bedrock layer with a short half-life *API*, such as API_{12}. These results indicate the bedrock contribution to rainwater storage. Although the bedrock layer can contribute as much to temporary rainwater storage during rainfall events as the soil layer (Fig. 15h), the water temporarily stored in the bedrock layer rapidly drains away. Subsequently, the bedrock layer still holds more water than the soil layer, which hardly drains.

Figure 16 also demonstrates the effect of root water uptake on water storage. The water storage in the soil layer dropped more rapidly in summer than in winter, indicating that water stored in the

soil layer was consumed by plants to a greater extent in summer. The water storage in the bedrock layer, on the other hand, did not exhibit such tendencies, suggesting that water stored in the bedrock layer is little influenced by transpiration. This conclusion is corroborated by Figs. 4 and 5, which show many roots contained in the soil layer and few in the bedrock layer.

4.4 Contribution of macropores and micropores to the bedrock water content

During rainfall events, the bedrock water content rose more sharply than that in the soil (Figs. 12 and 13), and the increments in the water content were comparable to, or even larger than, those in the soil layer (Fig. 15). After the end of rainfall events, both the water content and water storage in the bedrock dropped more rapidly and then varied less than those in the soil during the period without rain (Figs. 8, 12, 13, and 16). Figures 9 and 10 also demonstrate the very narrow range in which the bedrock water content was concentrated throughout the year, which resulted from the small variation in bedrock water content evident during the no-rainfall period.

These differences in water content and water storage dynamics between the soil and bedrock

may be explained by the differences in their water retention characteristics. In Fig. 17, we show the water retention curves of both the soil (15 and 30 cm deep from the ground surface; 100 cm^3) and bedrock (0-11 cm deep from the bedrock surface; 1860 cm^3) samples taken at the point indicated by a grey circle in Fig. 2 (Katsura *et al.*, 2006). Figure 17 shows that the soil water content continuously decreases with decreasing pressure head ψ throughout the measured ψ range, suggesting a broad pore radii distribution within the soils. The bedrock water content, on the other hand, gradually decreases with decreasing ψ in the range of ψ greater than approximately -70 cm and then changes little, taking the higher value than that in the soils at the low ψ values such as -200 cm. From these trends observed in the bedrock water retention curve, it can be inferred that the bedrock contains relatively clearly distinguishable macropores (i.e., pores which hold water in the range of $\psi >$ -70 cm) and micropores (i.e., pores which do not release water at $\psi =$ -200 cm). Such a bipolar pore radii distribution probably controls the water movement processes in the bedrock at the study site. During rainfall events, particularly with cumulative rainfall more than 15 mm (Figs. 14 and 15), rainwater infiltrates not only into micropores, most of which were already full of water prior to the event, but also into macropores, which generally hold little water before the event, causing an increase in the

water content comparable to that in the soils. After the events, the rainwater that infiltrated into the macropores drains away; therefore, the bedrock water content and water storage fall. The average water content (i.e., θ_{ave}) is higher in the bedrock than in the soil during a no-rainfall period (Fig. 16c) since the bedrock holds more water than the soil in the low ψ range (Fig. 17).

The bipolar pore system within the bedrock is reflected more clearly in rapid increase and decrease in the bedrock water content and water storage (Figs. 8, 12, 13, 16). While the soils, having a broader pore radii distribution (Fig. 17), produce a more gentle increase and decrease in the water content and water storage as rainwater infiltrates from smaller to larger pores and drains back gradually, rainwater infiltration into macropores in the bedrock and drainage from those produce almost instantaneous increase and decrease in them, respectively. During a no-rainfall period, micropores in the bedrock alone hold water for a long time, keeping the water content and water storage in the bedrock relatively steady.

The bipolar pore radii distribution within the bedrock discussed above may be derived from the bedrock weathering processes. In this study, bedrock water content was measured in the shallowest layer (0-11 cm deep from the bedrock surface), which has inevitably undergone the strongest effects

of weathering processes. In such highly weathered bedrock, it is possible that minerals with little resistance to weathering, such as feldspar, have been weathered into fine materials whereas other minerals still retain the original rock fabric and structure. Under such conditions, macropores can be produced after the fine materials derived from weathering of the former are dissolved and washed away whereas the latter forms micropores. In the deeper bedrock layer, which is weathered to less extent and may contain fractures, the different mechanism may control the water flow processes within the bedrock; this should be investigated in the next step.

It is difficult to determine whether the bipolar pore radii distribution in shallow bedrock mentioned here is true for bedrock in other headwater catchments or applies only to our study site, since little literature measuring water content variations in bedrock is available. Although Gimmi *et al*. (1997) measured changes in volumetric water contents in rock, their measurements were conducted on crystalline rock with extremely low porosity (<1%) during the desaturation process. It is very desirable that water content variations be further studied in highly weathered bedrock, which with high porosity can contribute substantially to hydrological processes in headwater catchments. Using coil-type TDR probes, such studies would contribute to a better understanding of water flow

processes in headwater catchments.

4.5 Definition of "bedrock" contributing to hillslope hydrological processes

Hillslope hydrology has conventionally drawn a distinction between "soil" and "bedrock", and believed that only the soil layer (i.e., the layer overlying the bedrock) contributes to hydrological processes in headwater catchments (e.g., Okimura *et al*., 1985; Hiramatsu *et al*., 1990). Ohta (1992) reported that the layer with saturated hydraulic conductivity less than 10^{-5} cm s^{-1} could be practically regarded as impermeable, and called the layer "hydrological bedrock". To determine the soil depth and the bedrock topography, cone penetration tests have been widely conducted (e.g., Ohta, 1988; Terajima and Moroto, 1990; Uchida *et al*., 2003a), and have established that bedrock be defined as the layer with the N_c value exceeding a threshold, taken as 50 for granitic regions (Okunishi and Iida, 1978; Okimura and Tanaka, 1980; Mochiduki and Matsumoto, 1986). Although the bedrock in our study site also had the N_c value greater than 50 and the conventional definition could be applied, the results of the water content measurements using the coil-type TDR probe definitely did not indicate

that the bedrock underlying the study site was impermeable, nor that it contributed little to hydrological phenomena in this headwater catchment. Moreover, the saturated hydraulic conductivity of the bedrock in the study site was 1.0×10^{-4} cm s^{-1} (Katsura *et al*., 2006), which also suggested that the bedrock could not be treated as impermeable. These findings obtained have demonstrated that cone penetration tests alone can determine neither "bedrock" nor hydrologically contributing layers. Also, the layer, even if it exhibits the N_c value exceeding the threshold defined for the geological region (Fig. 3) and is recognized as bedrock by visual estimation (Fig. 4), can carry and hold a substantial amount of water and therefore contribute substantially to hydrological processes in headwater catchments.

5 Conclusions

As a first step toward describing water movement processes in bedrock, we made a coil-type TDR probe capable of determining the volumetric water content in weathered bedrock at three depths. Whereas conventional TDR probes, with two or three long parallel rods (5-8 mm in

diameter), require drilling two or three accurately spaced guide holes into weathered bedrock, the large diameter (19 mm) of the coil-type TDR probe prepared in this study made it much easier to install the moisture sensors even into highly weathered bedrock. The calibration results for the individual sensors suggest that the values measured by the coil-type TDR probe are strongly dependent on water content in the surrounding medium.

The calibrated probe, together with commercially available profile soil moisture sensors, was installed in the bedrock and soil at a point in a granitic headwater catchment, and was used to monitor the water content profile for 1 year. Even rainfall events with relatively small cumulative rainfall of 15 mm increased both the soil and bedrock water contents, and the increment in the water content in the bedrock was comparable to, or even larger than, that in the soil. After the end of each rainfall event, the bedrock water content dropped more sharply than that in the soil, and then varied little during the period of no rainfall. As a result, bedrock water content was concentrated in a very narrow range throughout the year.

The water storage, calculated as the total water volume held within the soil and shallow bedrock layer, showed similar tendencies; the water storage in the bedrock rose in response to rainfall events,

and decreased more abruptly and varied less than that in the soil after these events.

All these observation results suggest that the bedrock water content, and therefore water movement processes in the bedrock in the study site, are controlled by clearly distinguished macropores and micropores contained in the bedrock. The sharp increase and decrease in the bedrock water content and water storage can be attributed to rainwater infiltration into and drainage from macropores in the bedrock.

In this study, we successfully measured the bedrock water content using the coil-type TDR probe. It can be concluded that the coil-type TDR probe is an effective and powerful tool to measure water content in weathered bedrock. This study revealed that bedrock, conventionally defined using the results of cone penetration tests and treated as an impermeable layer, does conduct and hold substantial amounts of water, and therefore contributes effectively to hydrological processes in headwater catchments. Spatial variability in the bedrock water contents and rainwater infiltration into still deeper bedrock layers should be investigated as a next step in order to describe water movement processes in the bedrock; this will make it possible to evaluate the effects of bedrock on runoff generation, water chemistry, and the occurrence of landslides in headwater catchments.

Acknowledgements

We wish to thank an anonymous reviewer for his helpful comments. We also thank D. Tsutsumi and H. Ando for their support during the field observations. This research was supported in part by a grant from the Fund of Monbusho for Scientific Research (16780114).

References

Anderson, S.P., Dietrich, W.E., Montgomery, D.R., Torres, R., Conrad, M.E., Loague, K., 1997a. Subsurface flow paths in a steep, unchanneled catchment. Water Resour. Res. 33:2637-2653.

Anderson, S.P., Dietrich, W.E., Torres, R., Montgomery, D.R., Loague, K., 1997b. Concentration-discharge relationships in runoff from a steep, unchanneled catchment. Water Resour. Res. 33:211-225.

Asano, Y., Uchida, T., Ohte, N., 2003. Hydrologic and geochemical influences on the dissolved silica concentration in natural water in a steep headwater catchment. Geochim. Cosmochim. Acta 67:1973-1989.

Burns, D.A., Murdoch, P.S., Lawrence, G.B., Michel, R.L., 1998. Effect of groundwater springs on NO_3^- concentrations during summer in Catskill Mountain streams. Water Resour. Res. 34:1987-1996.

Collaborative Research Group for the Granites around Lake Biwa, 2000. Granitic masses around Lake Biwa, southwest Japan: Part 5. The Tanakami Granite pluton. Earth Sci. 54:380-392 (in Japanese with English abstract).

Gimmi, T., Schneebeli, M., Flühler, H., Wydler, H., Baer, T., 1997. Field-scale water transport in unsaturated crystalline rock. Water Resour. Res. 33:589-598.

Handbook of Chemistry, 2004. Chemical Society of Japan, (Ed.), Maruzen, Tokyo (in Japanese†).

Hiramatsu, S., Mizuyama, T., Ishikawa, Y., 1990. Study of a method for predicting hillside landslides by analysis of transient flow of water in saturated and unsaturated soils. Shin-Sabo. 43:5-15 (in Japanese with English abstract).

Hokett, S.L., Chapman, J.B., Russell, C.E., 1992. Potential use of time domain reflectometry for measuring water content in rock. J. Hydrol. 138:89-96.

Inokura, Y., Yoshimura, K., 1992. Runoff and water quality characteristics of small streams in mountainous drainage basins in a water shortage period. Bull. Kyushu Univ. For. 66:31-44 (in Japanese with English abstract).

Kato, Y., Onda, Y., Mizuyama, T., Kosugi, K., Yoshikawa, A., Tsujimura, M., Hata, K., Okamoto, M., 2000. The difference of runoff peak response time in upstream of Ibi River underlain by different geology. J. Jpn. Soc. Erosion Contr. Eng. 53:38-43 (in Japanese with English abstract).

Katsura, S., Kosugi, K., Yamamoto, N., Mizuyama, T., 2006. Saturated and unsaturated hydraulic

conductivities and water-retention characteristics of weathered granitic bedrock. Vadose Zone J. 5:35-47 (Online).

Katsuyama, M., N. Ohte, and K. Kosugi. 2004. Hydrological control of the streamwater NO_3^- concentrations in a weathered granitic headwater catchment. (In Japanese, with English abstract) J. Jpn. For. Soc. 86(1):27-36.

Komatsu, Y., Onda, Y., 1996. Spatial variation in specific discharge of base flow in a small catchments, Oe-yama Region, Western Japan. J. Jpn. Soc. Hydrol. Water Resour. 9:489-497 (in Japanese with English abstract).

Kosugi, K., Katsura, S., Katsuyama, M., Mizuyama, T., 2006. Water flow processes in weathered granitic bedrock and their effects on runoff generation in a small headwater catchment. Water Resour. Res. 42: W02414. doi:10.1029/2005WR004275.

Kosugi, K., Tsutsumi, D., Mizuyama, T., Hasegawa, S., 2004. Combined penetrometer-moisture probe for measuring water content distribution in hillslope. J. Jpn. Soc. Erosion Contr. Eng. 57(3): 3-13 (in Japanese with English abstract).

Miyata, S., Uchida, T., Asano, Y., Ando, H., Mizuyama, T., 2003. Effects of bedrock groundwater

seepage on runoff generation at a granitic first order stream. J. Jpn. Soc. Erosion Contr. Eng. 56:13-19 (in Japanese with English abstract).

Mochiduki, M., Matsumoto, E., 1986. Behaviour of subsurface water in soil layers of a stream-head hollow. Bull. Environ. Res. Ctr. Univ. Tsukuba. 10:81-94 (in Japanese).

Montgomery, D.R., Dietrich, W.E., Heffner, J.T., 2002. Piezometric response in shallow bedrock at CB1: Implications for runoff generation and landsliding. Water Resour. Res. 38:1274. doi:10.1029/2002WR001429.

Montgomery, D.R., Dietrich, W.E., Torres, R., Anderson, S.P., Heffner, J.T., Loague, K., 1997. Hydrologic response of a steep, unchanneled valley to natural and applied rainfall. Water Resour. Res. 33:91-109.

Mulholland, P.J., 1993. Hydrometric and stream chemistry evidence of three storm flowpaths in Walker Branch Watershed. J. Hydrol. 151:291-316.

Nissen, H.H., Moldrup, P., Henriksen, K., 1998. High-resolution time domain reflectometry coil probe for measuring soil water content. Soil Sci. Soc. Am. J. 62:1203-1211.

Ohta, T., 1988. Storm runoff mechanism on forested slopes. J. Jpn. Soc. Hydrol. Water Resour.

1:75-82 (in Japanese with English abstract).

Ohta, T., 1992. Water cycle in hillslope. In: Tsukamoto, Y. (Ed.), Forest Hydrology, Buneido, Tokyo, pp. 125-157 (in Japanese†).

Okimura, T., Ichikawa, R., Fujii, I., 1985. Methods to predict failures on granite mountain slopes by a infiltrated water movement model in a surface layer. Shin-Sabo. 37:4-13 (in Japanese with English abstract).

Okimura, T., Tanaka, S., 1980. Researches on soil horizon of weathered granite mountain slope and failured surface depth in a test field. Shin-Sabo 116:7-16 (in Japanese with English abstract).

Okunishi, K., Iida, T., 1978. Study on the landslides around Obara Village, Aichi Prefecture (I)-Interrelationship between slope morphology, subsurface structure and landslides-. Bull. Disast. Prevent. Res. Instit. 21B:297-311 (in Japanese with English abstract).

Onda, Y., Komatsu, Y., Tsujimura, M., Fujihara, J., 1999. Possibility for predicting landslide occurrence by analyzing the runoff peak response time. J. Jpn. Soc. Erosion Contr. Eng. 51:48-52 (in Japanese).

Onodera, S., 1991. Subsurface water flow in the multi-layered hillslope. Geogr. Rev. Jpn.

64A:549-568 (in Japanese with English abstract).

Robinson, D.A., Jones, S.B., Wraith, J.M., Or, D., and Friedman, S.P., 2003. A review of Advances in dielectric and electrical conductivity measurement in soils using time domain reflectometry. Vadose Zone J. 2:444-475 (Online).

Roth, K., Schulin, R., Flühler, H., Attinger, W., 1990. Calibration of time domain reflectometry for water content measurement using a composite dielectric approach. Water Resour. Res. 26:2267-2273.

Sasaki, T., Sugihara, K., Adachi, T., Nishida, K., Lin, W., 1998. Application of time domain reflectometry to determination of volumetric water content in rock. Water Resour. Res. 34:2623-2631.

Schneebeli, M., Flühler, H., Gimmi, T., Wydler, H., Läser, H.P., Baer, T., 1995. Measurements of water potential and water content in unsaturated crystalline rock. Water Resour. Res. 31:1837-1843.

Suzuki, M., Kobashi, S., 1981. The critical rainfall for the disasters caused by slope failures. Shin-Sabo. 121:16-26 (in Japanese with English abstract).

1 Terajima, T., Mori, A., Ishii, H., 1993. Comparative study of deep percolation amount in two small
2 catchments in granitic mountain. Jpn. J. Hydrol. Sci. 23:105-118 (in Japanese with English
3 abstract).
4 Terajima, T., Moroto, K., 1990. Stream flow generation in a small watershed in granitic mountain.
5 Trans. Jpn. Geomorphol. Union. 11:75-96 (in Japanese with English abstract).
6 Topp, G.C., Davis, J.L., Annan, A.P., 1980. Electromagnetic determination of soil water content:
7 Measurements in coaxial transmission lines. Water Resour. Res. 16:574-582.
8 Torii, A., 1996. Development of immature soils after afforestation on bare hills, with special
9 reference to their mineralogical changes. Jpn. J. Environ. 38:53-61 (in Japanese with English
10 abstract).
11 Tsutsumi, D., 2003. Study on root system development by modeling approach. Ph. D. thesis. Kyoto
12 University, Kyoto, Japan: 136pp.
13 Uchida, T., Asano, Y., Ohte, N., Mizuyama, T., 2003a. Analysis of flowpath dynamics in a steep
14 unchannelled hollow in the Tanakami Mountains of Japan. Hydrol. Process. 17:417-430.
15 Uchida, T., Asano, Y., Ohte, N., Mizuyama, T., 2003b. Seepage area and rate of bedrock groundwater

discharge at a granitic unchanneled hillslope. Water Resour. Res. 39:1018. doi:10.1029/2002WR001298.

Vaz, C.M.P., Hopmans, J.W., 2001. Simultaneous measurement of soil penetration resistance and water content with a combined penetrometer-TDR moisture probe. Soil Sci. Soc. Am. J. 65:4-12.

Wilson, C.J., Dietrich, W.E., 1987. The contribution of bedrock groundwater flow to storm runoff and high pore pressure development in hollows. In: R.L. Beschta *et al*. (Eds.), Erosion and sedimentation in the Pacific Rim. Publ. No. 165, Int. Assoc. of Hydrol. Sci., Gentbrugge, Belgium, pp. 49-59.

† The title or source is a tentative translation by the authors from the original.

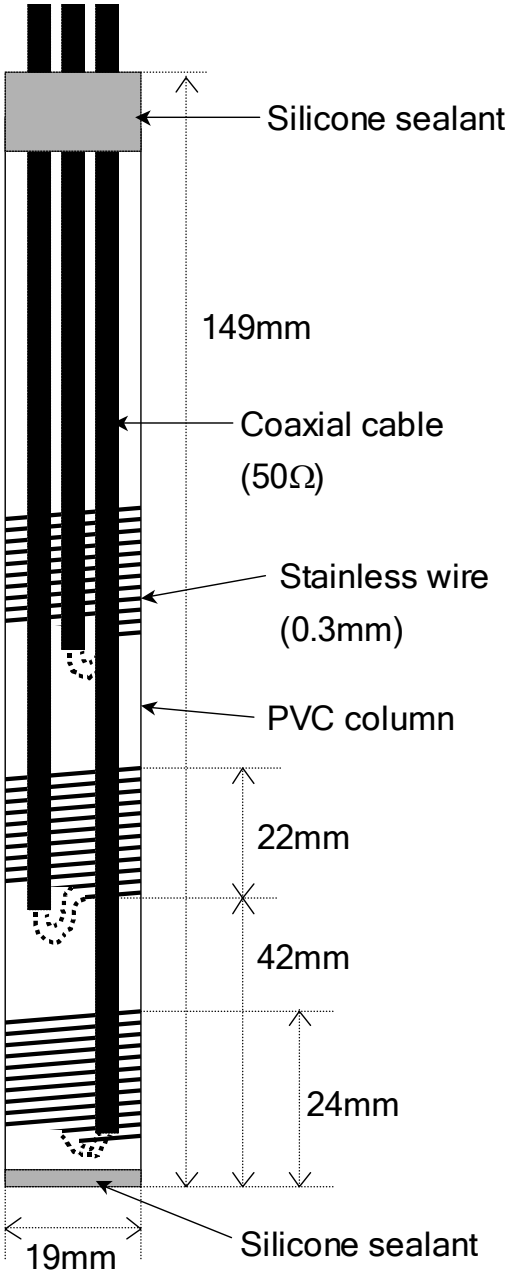

Fig. 1. Detailed diagram of the coil-type TDR probe.

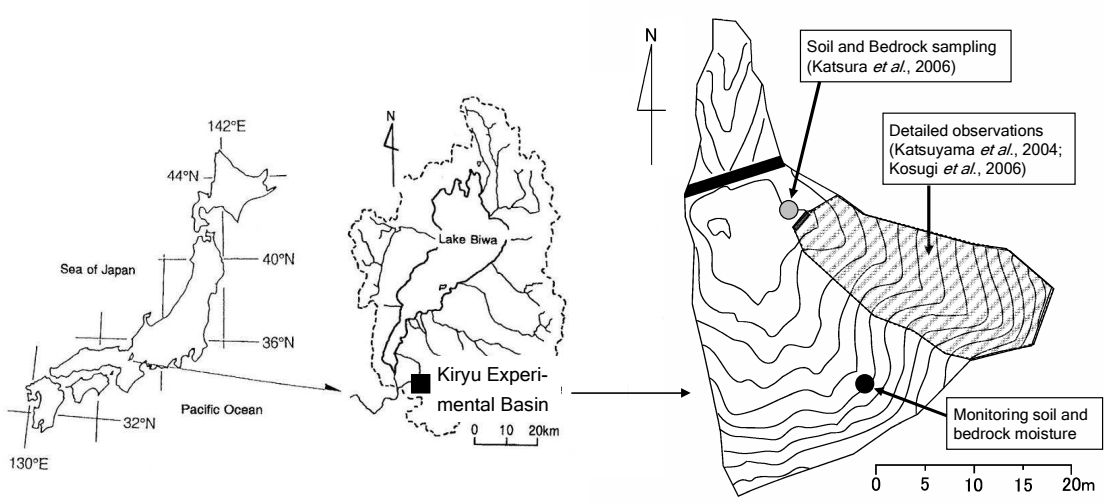

Fig. 2. Maps of Japan (left), Shiga Prefecture (central), and the Akakabe catchment (right). The point at which the moisture sensors and probes were installed is indicated by a solid circle. The unchanneled catchment in which Katsuyama *et al*. (2004) and Kosugi *et al*. (2006) conducted detailed observations and the point at which Katsura *et al*. (2006) took soil and bedrock samples for hydraulic properties determination are also shown. The map of the Akakabe catchment has a contour interval of 1 m.

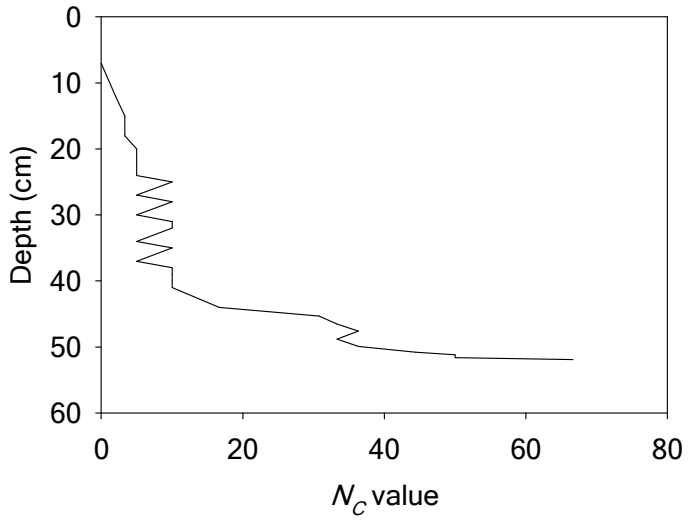

Fig. 3. Change of the N_C value with depth at the water content measurement point.

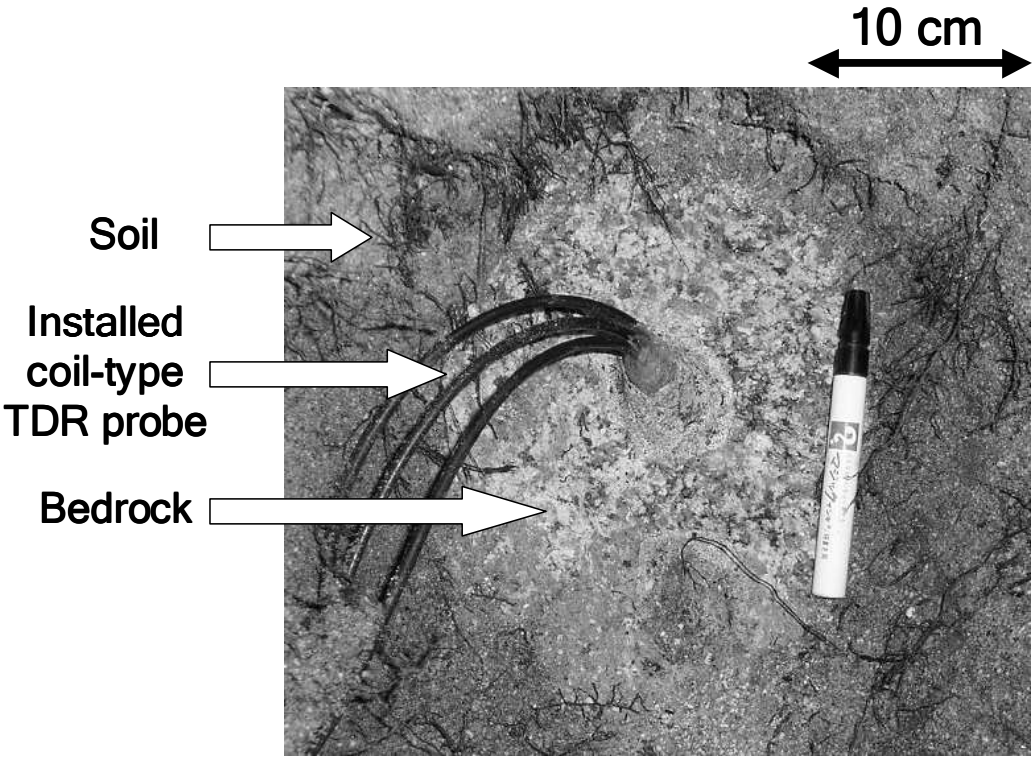

Fig. 4. Photograph around the soil-bedrock interface. The installed coil-type TDR probe is also included.

Fig. 5. Photograph of the coil-type TDR probe installed in the bedrock.

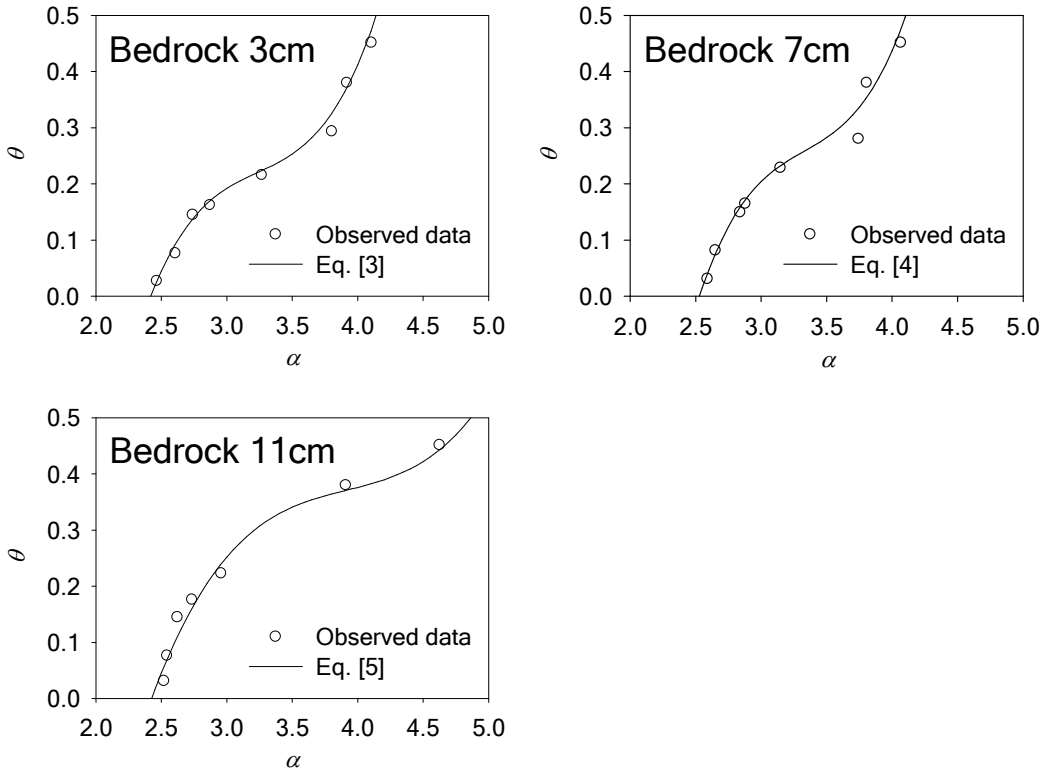

Fig. 6. Calibration results of the coil-type TDR probe (open circles) and fitted third-order polynomial Eqs. [3]-[5] (solid lines).

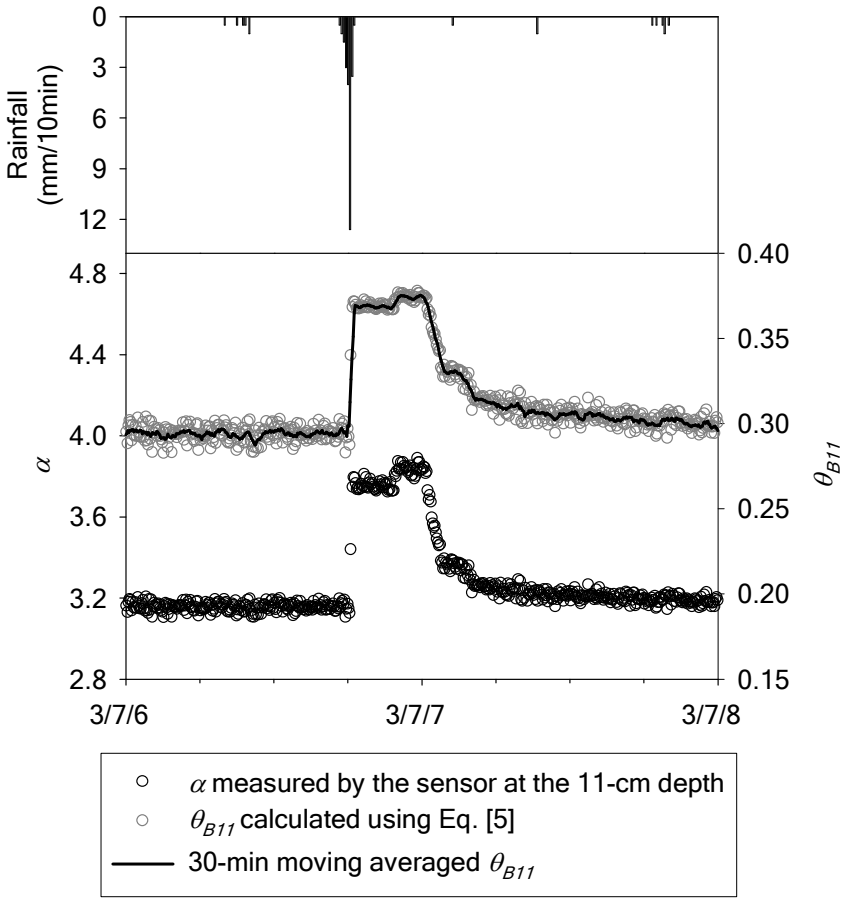

Fig. 7. Processes of calculating the water content θ from the measured value α. Here we show the process of calculating θ_{B11} as an example.

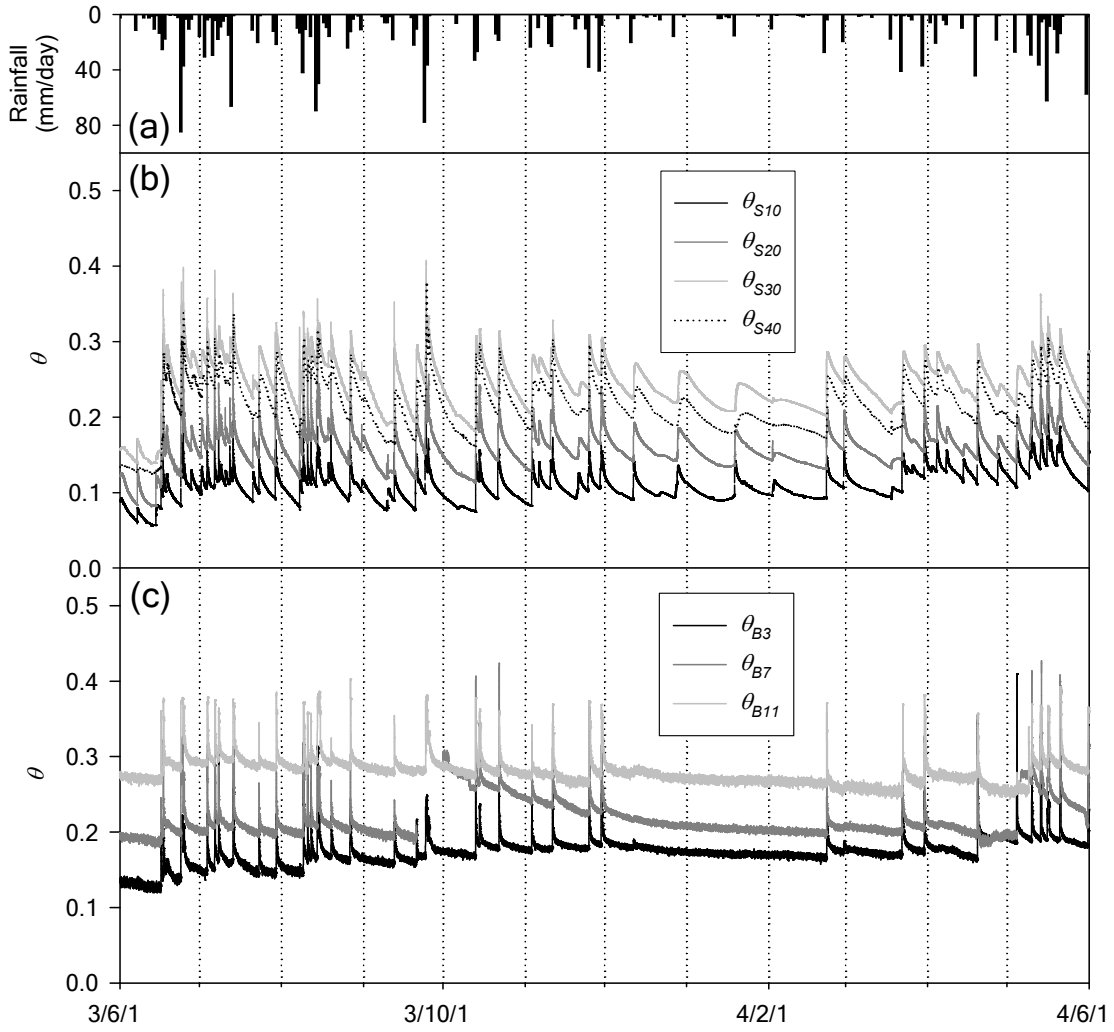

Fig. 8. (a) Hyetograph, and the annual variation in the water contents in (b) the soil and (c) the bedrock throughout the observation period. The date is expressed in year/month/day. Note that θ_{B7} has no data from 2003/9/21 through 2003/9/30 and on 2004/5/13 because the sensor was not functional.

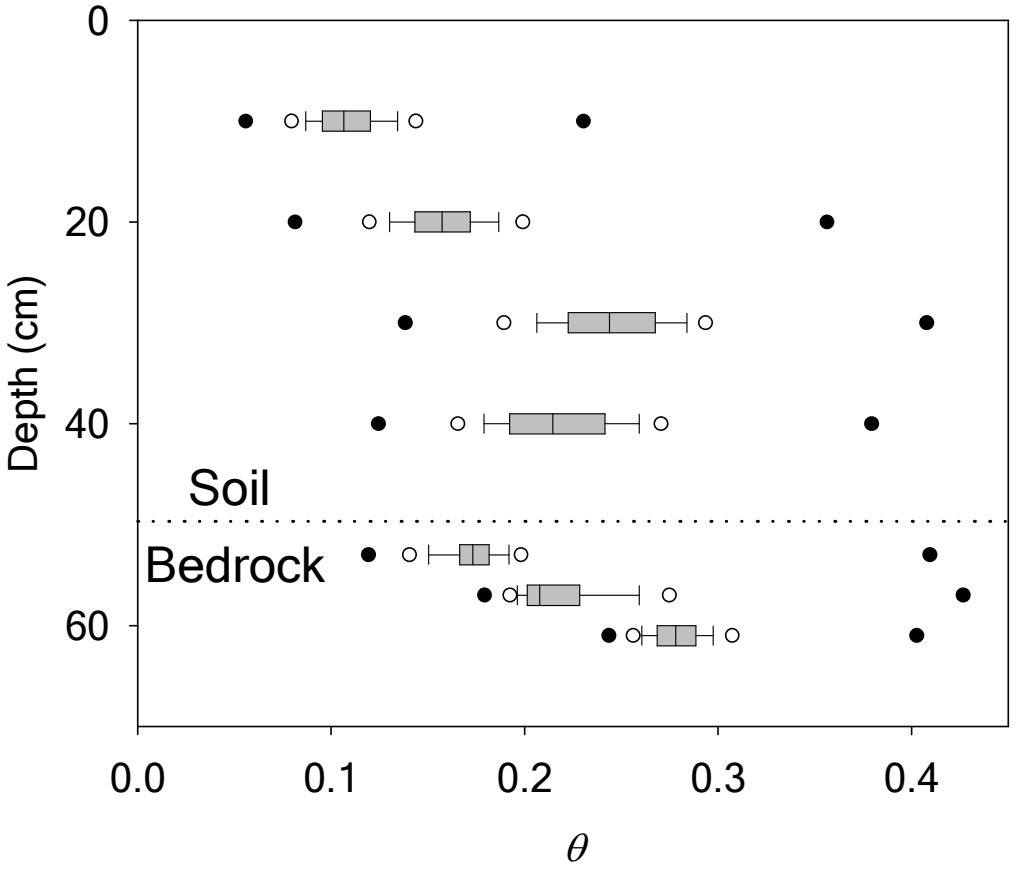

Fig. 9. Variations in the water contents in both the soils and bedrock. The sides of the box closest to and farthest from zero indicate 25th and 75th percentiles, respectively, and the line within the box denotes the median. The whiskers to the left and right of the box represent the 10th and 90th percentiles, respectively. The open circles closest to and farthest from zero indicate the 5th and 95th percentiles, and the solid circles denote the minimum and maximum, respectively.

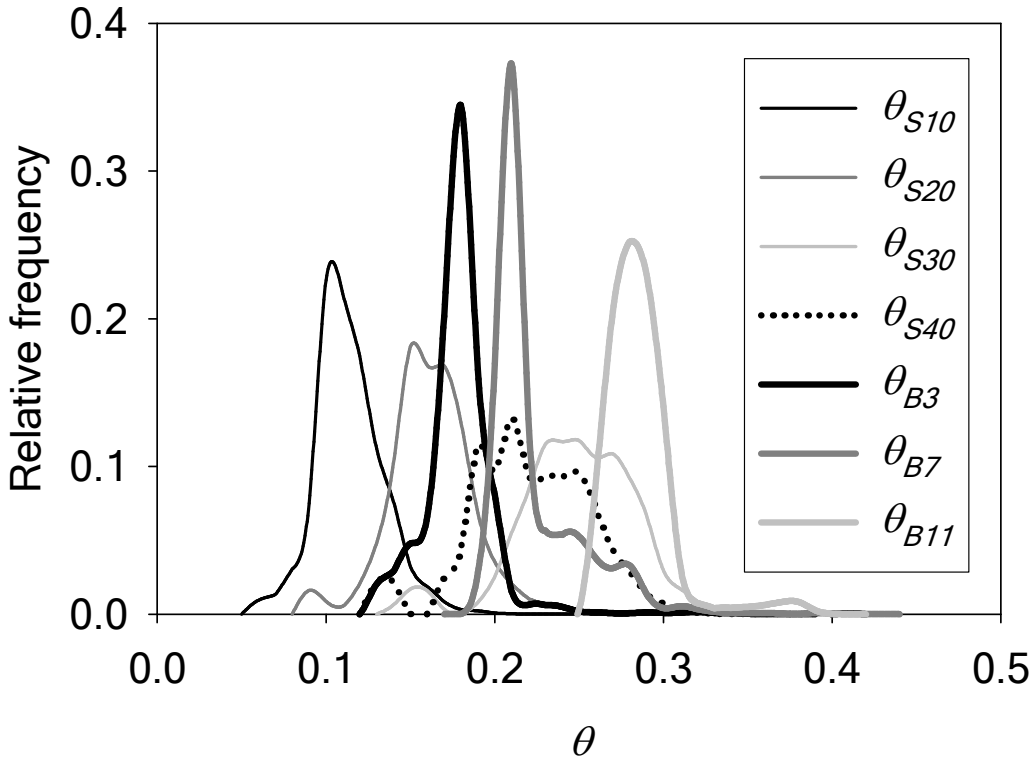

Fig. 10. Relative frequency of the water content at each depth observed throughout the observation period.

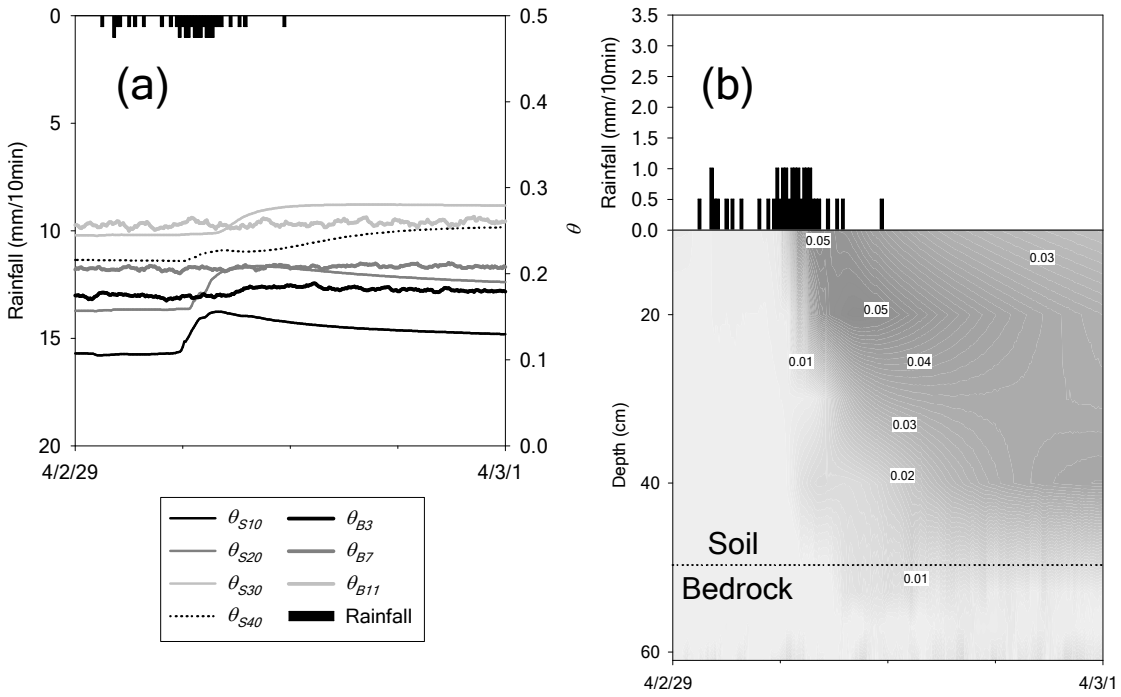

Fig. 11. (a) Temporal variations in the water content and (b) the contour lines of the increments in the water content compared to those at the beginning of rainfall from the soil through the bedrock observed during a small rainfall event on 2004/2/29.

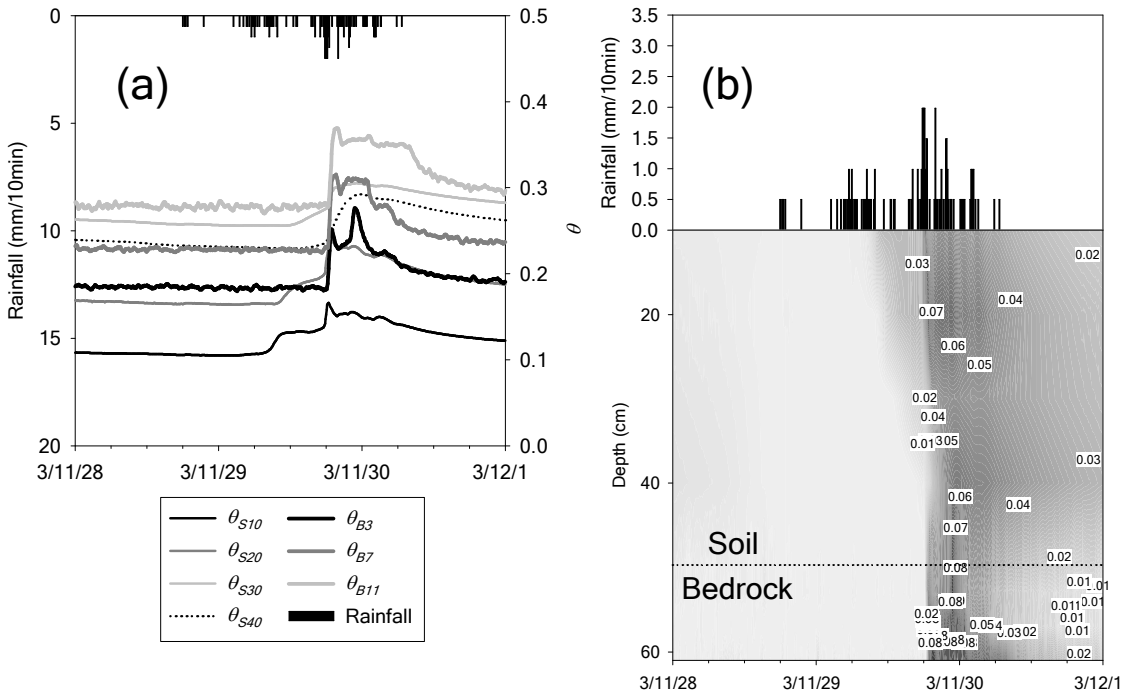

Fig. 12. (a) Temporal variations in the water content and (b) the contour lines of the increments in the water content compared to those at the beginning of rainfall from the soil through the bedrock observed during a medium-sized rainfall event from 2003/11/28 through 2003/11/30.

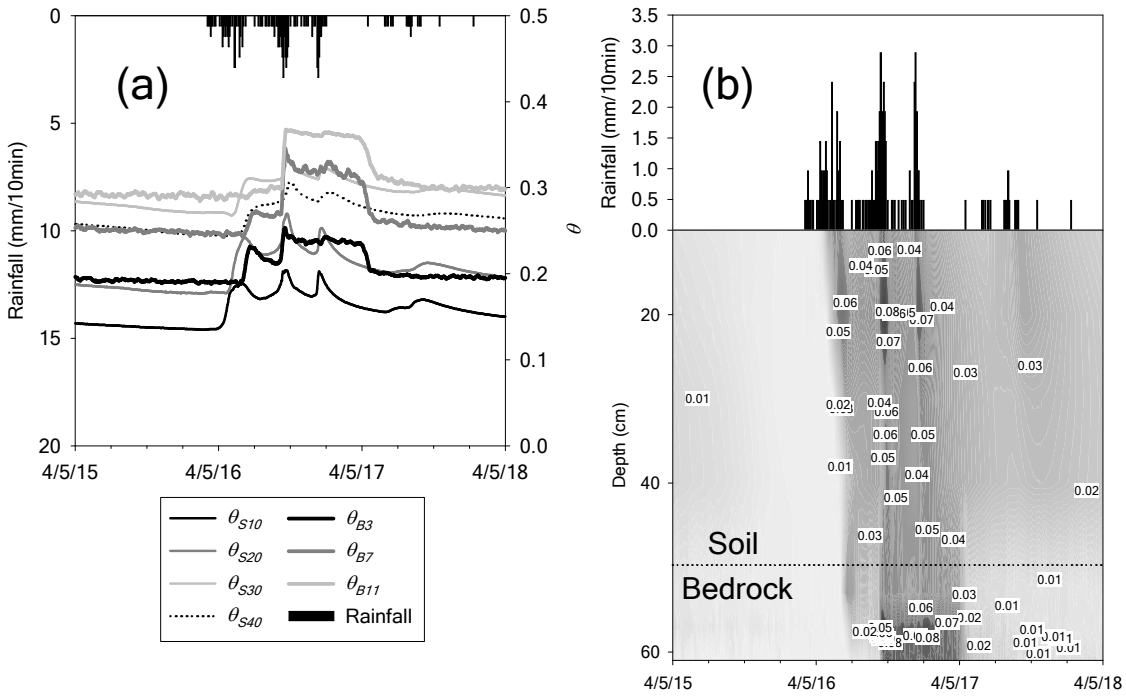

Fig. 13. (a) Temporal variations in the water content and (b) the contour lines of the increments in the water content compared to those at the beginning of rainfall from the soil through the bedrock observed during a large rainfall event from 2004/5/15 through 2004/5/17.

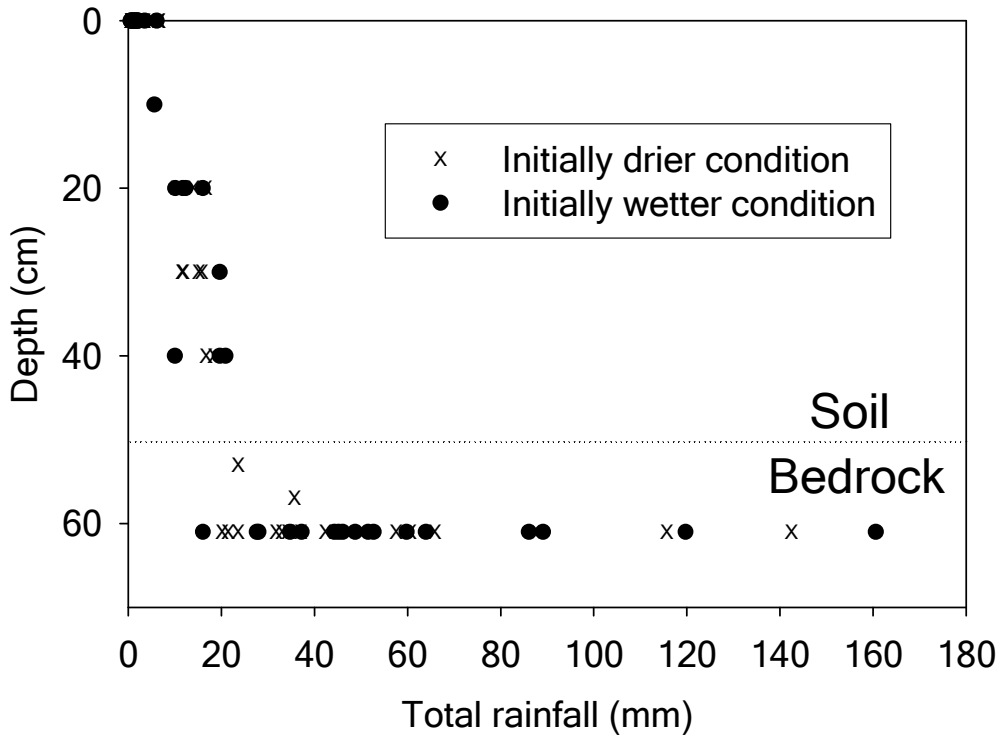

Fig. 14. Relationship between the maximum depth that showed more than 0.03 increment in the water content compared to that at the event initiation and the total rainfall observed in the event. The plot was classified into two groups according to θ_{S10} at rainfall initiation; the initially drier condition implies lower water content in the surface soil layer (θ_{S10}<0.1) than the initially wetter condition (θ_{S10}>0.1) at the commencement of the event.

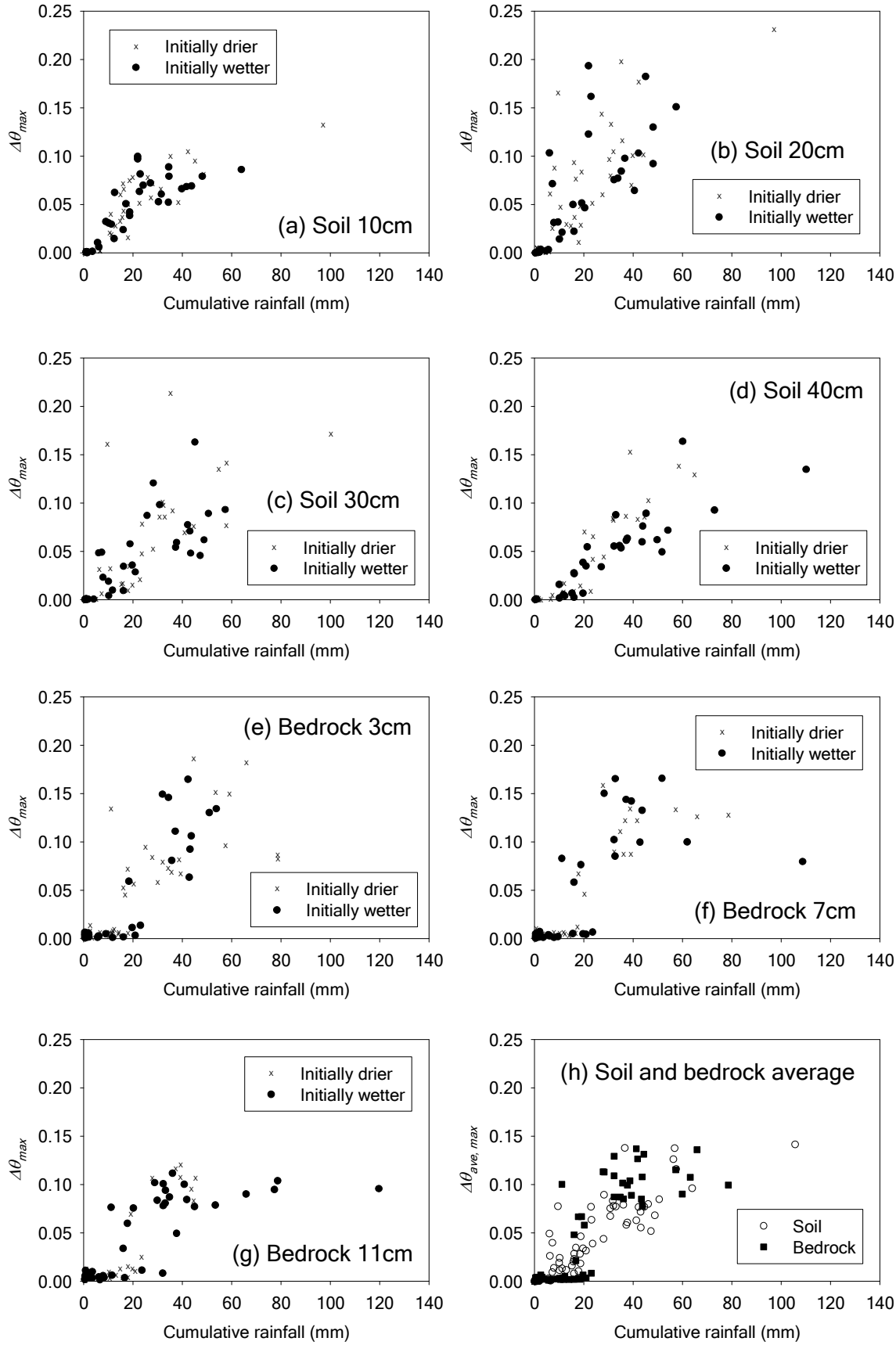

Fig. 15. Relationships between $\Delta\theta_{max}$ and the cumulative rainfall observed before the maximum water content was observed (a-g) at each depth and (h) in the whole soil and bedrock layer. The plot in Fig. 15a-g was classified into two groups according to the water content at the beginning of rainfall at each depth by a method similar to that in Fig. 14. Fig. 15h shows the values of $\Delta\theta_{max}$ averaged over the 50-cm-thick soil layer and the 13-cm-thick bedrock layer ($\Delta\theta_{ave,\ max}$).

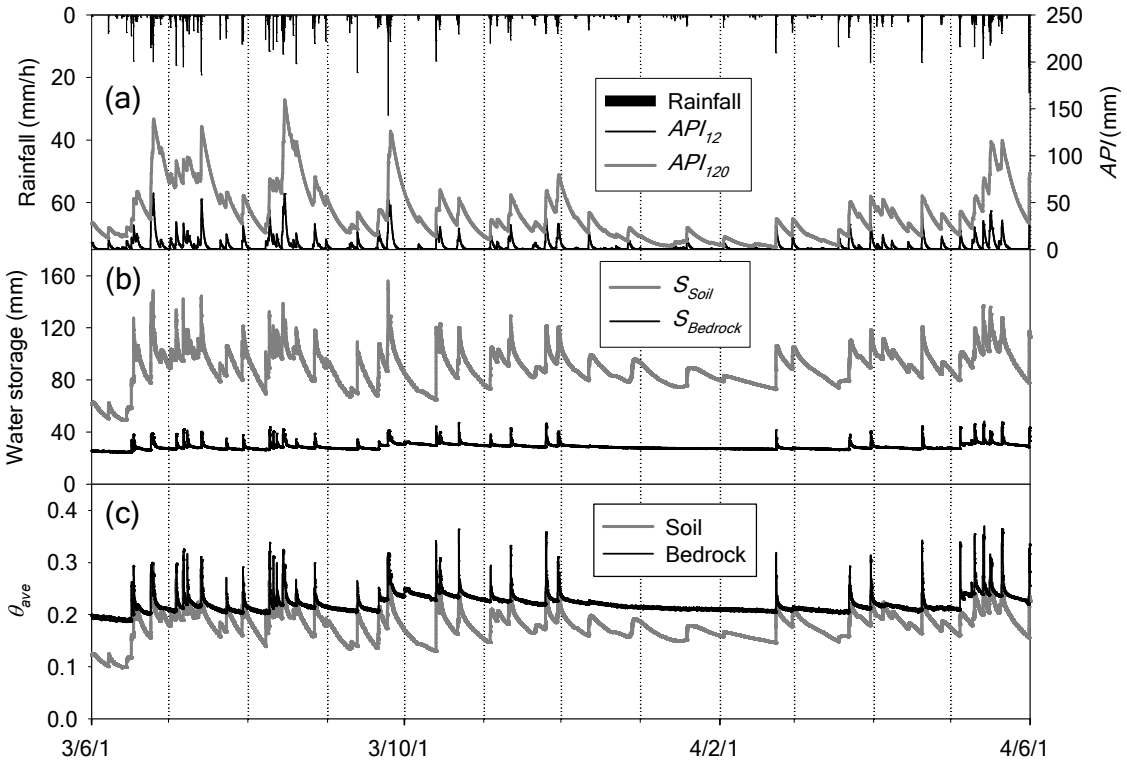

Fig. 16. (a) Hyetograph, including the annual variations in API_{12} and API_{120}, and the annual variations in (b) the water storage in the soil and bedrock (S_{Soil} and $S_{Bedrock}$, respectively) and (c) the average water content in the 50-cm-thick soil layer and the 13-cm-thick bedrock layer.

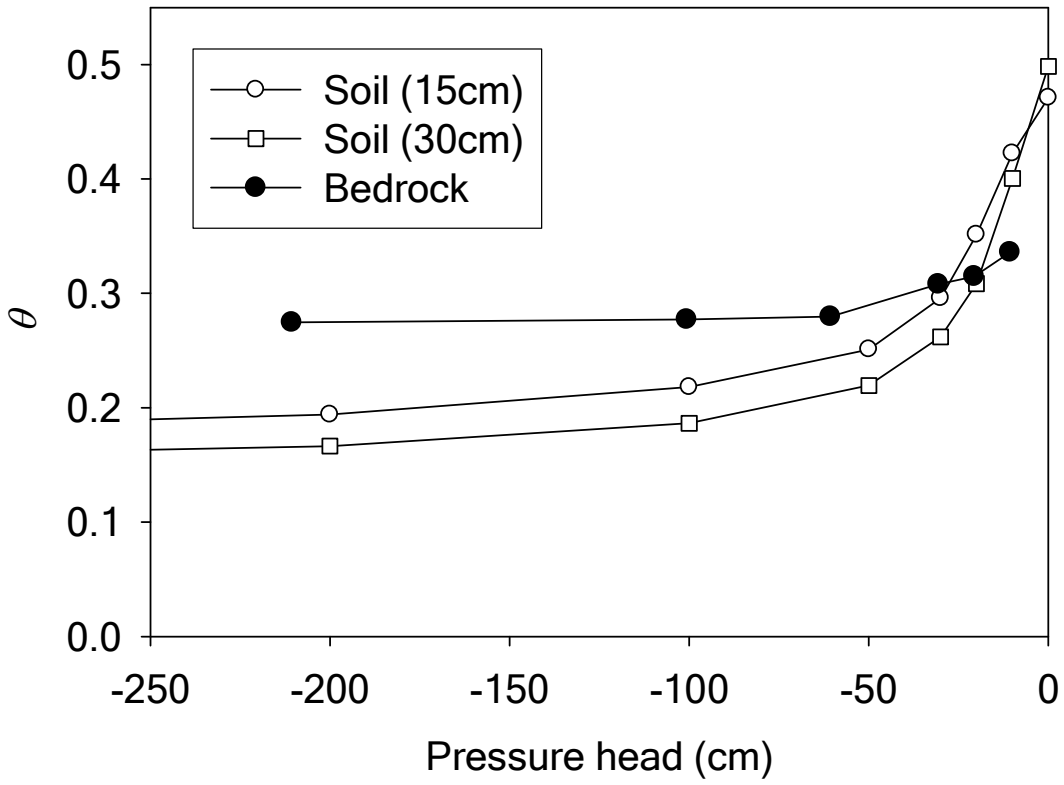

Fig. 17. Water retention curves of the soil (15 and 30 cm deep from the ground surface) and shallow bedrock (0-11 cm deep from the bedrock surface) samples taken at the point indicated by a grey circle in Fig. 2 (Katsura *et al.*, 2006).